Impulsive Noise Mitigation for Wireless OFDM

Paolo Banelli and Luca Rugini
Department of Engineering
University of Perugia
Perugia, Italy
{paolo.banelli, luca.rugini}@unipg.it

***Abstract*—Impulsive noise typically represents a man-made disturbance that, although it may impair any electrical device, is often neglected in the performance analysis of wireless communication systems. This paper exploits some recent results on Bayesian estimators of Gaussian sources impaired by Middleton Class-A noise, in order to investigate the usefulness of such estimators for orthogonal frequency-division multiplexing (OFDM)-based wireless communications. Specifically, this paper extends the use of minimum mean-squared error (MMSE) and maximum signal-to-noise-ratio (SNR) estimators to OFDM systems in frequency-selective fading channels, and compares the associated gain in symbol-error rate (SER) performance.**

Keywords—Blanker, Class-A noise, impulsive noise, MMSE estimation, soft limiter.

I. INTRODUCTION

Impulsive noise is a quite common source of disturbance to telecommunication systems, typically generated by electrical engines, appliances, and switches, which may randomly impair both wireless and wired communications. Basically, impulsive noise is an interference that randomly adds up to the underlying Gaussian thermal noise. A simple way to model the random presence and absence of this interference makes use of a Bernoulli-Gaussian model, i.e., a two-state conditional probability density function (pdf) of the overall noise, represented by the mixture of two Gaussian functions [1]–[3]. The Middleton's Class-A noise is a more general and largely accepted canonical model, which captures the statistical behavior of a wider class of impulsive interference, by resorting to a mixture of virtually infinite Gaussian functions, with Poisson distributed weights [4]–[9].

The widespread use of orthogonal frequency-division multiplexing (OFDM) techniques in digital communications has spurred some investigation on the effects of impulsive interferences modeled as a Class-A noise, and on its countermeasures, both in wired [10]–[14] and wireless [3]–[5], [15]–[17] OFDM-based systems. Among the receiver techniques specifically tailored to face such interference, it is possible to distinguish between two categories: simple instantaneous devices, which try to limit the effect of impulsive interference on a sample-by-sample basis [3]–[6], [10], [11], and more complex methods, generally iterative and data-aided, which try to reconstruct and jointly subtract the impulsive noise to the entire OFDM block [13]–[18]. This paper belongs to the first category of possible receivers, which are worth to be investigated alone, as well as a first stage of the more complex iterative receivers. In this framework, for wireless OFDM system impaired by RF impulsive noise, [3]–[5] proposed sample-based receivers, which may simply clip, null, or both clip and null, the envelope of the complex baseband received signal, when it overpasses some given thresholds. Similar receivers have been analyzed also in [10], [11], [19], and [20]. All the thresholds and parameters of these simple receivers are typically optimized to maximize their output signal-to-noise ratio (SNR).

Recently, [6] proposed instantaneous receivers for a real Gaussian source impaired by a real Class-A baseband impulsive noise, which may model OFDM-based wired communications, such as ADSL and power-line communications. Furthermore [6], by proposing to consider the mean-squared error (MSE) at the receiver output, not only optimized in a minimum MSE (MMSE) sense the thresholds of the clipping and blanking nonlinearities, but also derived the global MMSE sample-based receiver. The MMSE criterion is not equivalent to the maximum-SNR (MSNR) criterion in non-Gaussian noise environments [21], and it is actually slightly suboptimal from the error probability viewpoint. However, since the global MSNR receiver is not known, the global MMSE receiver may outperform, in terms of SNR, some suboptimal receivers (e.g., clippers and blankers) whose thresholds and parameters have been optimized in an MSNR sense.

This paper provides the following contributions. First, we propose to apply the MMSE estimators derived in [6] to the real and imaginary part of the complex baseband signal of a wireless OFDM system, which we call Cartesian receivers, in contrast to the polar receivers in [3]–[5], [10], [11]. Second, we extend to complex signals the real MMSE estimator in [6], which turns out to be a polar receiver. Third, we propose to adapt, before equalization, the nonlinear receivers to the change of the frequency-selective fading channel that typically affects OFDM wireless transmissions. This is different from [3], which first equalizes the channel and successively contrasts the impulsive noise by a nonlinear device, and from [2], [4], [5], and [20], which consider a nonrealistic frequency-flat channel. Fourth, we compare by simulations the symbol error rate (SER) performance of several receivers in frequency-selective fading channels. Besides, we propose a semi-analytical SER theoretical analysis, which turns out to be quite accurate.

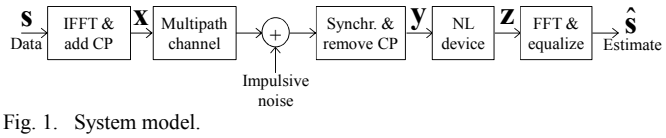

Fig. 1. System model.

978-1-4799-1931-4/15/$31.00 ©2015 IEEE

II. System Model

A. Transmitter

We consider the OFDM system of Fig. 1, with N subcarriers and cyclic prefix (CP) of length L. We denote the generic OFDM data block by $\mathbf{s}=[s[0],...,s[N-1]]^T$, where $s[n]$ is the M-QAM (or M-PSK) symbol transmitted in the n th subcarrier, and N is the number of subcarriers. We assume that the symbols $\{s[n]\}$ are independent and have zero mean, with variance $\sigma_s^2=E\{|s[n]|^2\}$. After IFFT of size N, a CP of size L is appended, where L is the maximum channel order. The transmitted signal can be expressed by [22]

$$\mathbf{x}=\mathbf{T}_{\mathrm{CP}}\mathbf{F}^H\mathbf{s}, \tag{1}$$

where $\mathbf{F}$ is the N-size unitary DFT matrix, $\mathbf{T}_{\mathrm{CP}}=[\mathbf{J}^T\ \mathbf{I}_N]^T$ is the $P\times N$ CP insertion matrix, where $P=N+L$, and $\mathbf{J}$ contains the last L rows of $\mathbf{I}_N$.

B. Channel Model

The frequency-selective multipath channel is modeled as a linear time-invariant FIR filter, by $\mathbf{h}=[h[0],...,h[L]]^T$, where $h[l]$ is the l th discrete-time path of the channel. We assume that the paths $\{h[l]\}$ are independent and have zero mean, with variance $\sigma_l^2=E\{|h[l]|^2\}$. We define $\sigma_h^2=\sum_{l=0}^{L}|h[l]|^2$, the $P\times P$ Toeplitz time-domain channel matrix $\mathbf{H}_0=\mathrm{Toep}_P(\mathbf{h})$, with first column expressed by $[h[0],...,h[L],0,...,0]^T$, the $N\times N$ circulant time-domain channel matrix $\mathbf{H}=\mathbf{R}_{\mathrm{CP}}\mathbf{H}_0\mathbf{T}_{\mathrm{CP}}$, where $\mathbf{R}_{\mathrm{CP}}=[\mathbf{0}_{N\times L}\ \mathbf{I}_N]$ is the $N\times P$ CP removal matrix, and the $N\times N$ diagonal frequency-domain channel matrix $\mathbf{\Lambda}=\mathbf{F}\mathbf{H}\mathbf{F}^H$. From (1), the $N\times 1$ time-domain received signal, after synchronization and CP removal, is expressed by [22]

$$\mathbf{y}=\mathbf{R}_{\mathrm{CP}}\mathbf{H}_0\mathbf{x}+\mathbf{w}=\mathbf{H}\mathbf{F}^H\mathbf{s}+\mathbf{w}, \tag{2}$$

where $\mathbf{w}=[w[0],...,w[N-1]]^T$ is the impulsive noise vector.

C. Impulsive Noise Model

The noise $\mathbf{w}=[w[0],...,w[N-1]]^T$ in (2) is modeled as a complex white Class-A noise [8], [9] with zero mean and variance $\sigma_w^2=E\{|w[n]|^2\}$. Using $w[n]=w_r[n]+jw_j[n]$, where $w_r[n]=\mathrm{Re}\{w[n]\}$ and $w_j[n]=\mathrm{Im}\{w[n]\}$, the joint pdf of $(w_r[n],w_j[n])$ is expressed by

$$f_{w_r,w_i}(w_r,w_i)=\sum_{m=0}^{\infty}\frac{\beta_m}{\pi\sigma_m^2}e^{-(w_r^2+w_i^2)/\sigma_m^2}, \tag{3}$$

where m is the random number of noise sources that are active, with Poisson distributed probability $\Pr\{m\}=\beta_m=e^{-A}A^m/(m!)$, and $A=E\{m\}=\sum_{m=0}^{\infty}m\beta_m$ is the expected value of the number of active sources [9]. The total noise power σ_w^2 is the sum of the power σ_t^2 of the Gaussian part and of the power σ_I^2 of the impulsive part, as expressed by $\sigma_w^2=\sigma_t^2+\sigma_I^2$, and hence, by defining the Gaussian-to-Class-A noise ratio $T=\sigma_t^2/\sigma_I^2$, we have $\sigma_m^2=\sigma_w^2(T+m/A)/(T+1)$. This means that (3) is specified only by the three parameters A, T, and σ_w^2 [9]. This paper assumes that the noise parameters are perfectly known at the receiver, as well as the received signal power $\sigma_y^2=\sigma_h^2\sigma_s^2+\sigma_w^2$ and the channel matrix $\mathbf{H}$.

D. Receiver

We assume that the receiver is the cascade of two blocks: an instantaneous nonlinear device $g(\cdot)$, to be designed, that reduces the impulsive noise in the time domain, and a subsequent linear operator that performs FFT and channel equalization. By applying the nonlinear device to (2), the received samples can be expressed by $z[n]=g(y[n])$, and, by collecting the samples in $\mathbf{z}=[z[0],...,z[N-1]]^T$, the channel equalizer yields the soft data estimate as

$$\hat{\mathbf{s}}=K^{-1}\mathbf{\Lambda}^{-1}\mathbf{F}\mathbf{z}, \tag{4}$$

where K is the average gain of the nonlinear device $g(\cdot)$. The following section explains how to design the nonlinear device $g(\cdot)$ and how to calculate the average gain K.

III. Impulsive Noise Mitigation

To design the nonlinear device that performs the noise reduction, we may follow either the Bayesian MMSE criterion or the MSNR criterion. Moreover, to simplify the receiver, we may assume a Cartesian nonlinear device that acts independently on the real part and on the imaginary part of the received signal in (2). This is clearly suboptimal, because the Class-A impulsive noise in-phase and quadrature (I/Q) components are not independent, as clearly shown by (3). Actually, the dependence of (3) on the noise envelope, and not on the phase, seems to suggest to use polar receivers, which jointly acts on the I/Q components by a nonlinear device that distorts the received signal envelope, leaving unchanged the phase.

A. Cartesian Bayesian MMSE Estimator

First, we rewrite (2) as

$$\mathbf{y}=\mathbf{v}+\mathbf{w}, \tag{5}$$

where $\mathbf{v}=\mathbf{H}\mathbf{F}^H\mathbf{s}$ is the noiseless version of $\mathbf{y}$, and then as

$$\overline{\mathbf{y}}=\overline{\mathbf{v}}+\overline{\mathbf{w}}, \tag{6}$$

where $\overline{\mathbf{y}}=[\overline{y}[0],...,\overline{y}[2N-1]]^T=[\mathrm{Re}\{\mathbf{y}^T\},\mathrm{Im}\{\mathbf{y}^T\}]^T$,

$$\overline{\mathbf{v}}=[\overline{v}[0],...,\overline{v}[2N-1]]^T=[\mathrm{Re}\{\mathbf{v}^T\},\mathrm{Im}\{\mathbf{v}^T\}]^T, \tag{7}$$

$$\overline{\mathbf{w}}=[\overline{w}[0],...,\overline{w}[2N-1]]^T=[\mathrm{Re}\{\mathbf{w}^T\},\mathrm{Im}\{\mathbf{w}^T\}]^T. \tag{8}$$

Our aim is to determine the function $g_c(\cdot)$ that minimizes the MSE J, defined as

$$J=E\{|g(\overline{y}[n])-\overline{v}[n]|^2\}. \tag{9}$$

Since $\overline{v}[n]$ and $\overline{w}[n]$ are independent, the MMSE estimator of $\overline{v}[n]$, e.g., $g_c(\overline{y}[n])=E\{\overline{v}[n]|\overline{y}[n]\}$, is expressed by [6]

$$g_c(\overline{y}[n])=\frac{\int_{-\infty}^{\infty}\overline{v}[n]f_{\overline{w}[n]}(\overline{y}[n]-\overline{v}[n])f_{\overline{v}[n]}(\overline{v}[n])d\overline{v}[n]}{f_{\overline{y}[n]}(\overline{y}[n])}, \tag{10}$$

where $f_{\overline{v}[n]}(\overline{v}[n])$, $f_{\overline{w}[n]}(\overline{w}[n])$, and $f_{\overline{y}[n]}(\overline{y}[n])$ are the pdfs of $\overline{v}[n]$, $\overline{w}[n]$, and $\overline{y}[n]$, respectively.

In order to determine $g_c(\cdot)$ in (10), we have to calculate the pdfs of $\overline{v}[n]$, $\overline{w}[n]$, and $\overline{y}[n]$. For what concerns the pdf of $\overline{v}[n]$, we note that $\mathbf{v}=\mathbf{H}\mathbf{F}^H\mathbf{s}$ is obtained from IFFT of data, followed by linear filtering. If the number of subcarriers N is sufficiently high, e.g., $N\geq 64$, the time-domain signal $\mathbf{F}^H\mathbf{s}$ can be approximated as stationary Gaussian with zero mean and variance σ_s^2, by the Central Limit Theorem. After linear filtering performed by the multipath channel, the time-domain signal $v[n]$ is still zero-mean Gaussian, but with modified variance $\sigma_v^2=\sigma_h^2\sigma_s^2$. Hence, for practical OFDM systems with large N, $\overline{v}[n]$ can be well approximated as zero-mean Gaussian with variance $\sigma_{\overline{v}}^2=\sigma_v^2/2$ on each I/Q component.

The pdf of $\overline{w}[n]$, obtained from marginalization of (3), is

$$f_{\overline{w}}(\overline{w}[n]) = \sum_{m=0}^{\infty} \frac{\beta_m}{\sqrt{\pi\sigma_m^2}} e^{-\overline{w}^2[n]/\sigma_m^2}, \quad (11)$$

leading to a real-valued white Class-A noise with the same A and T of $w[n]$, but with halved variance $\sigma_{\overline{w}}^2 = \sigma_w^2/2$.

Since the signal $\overline{v}[n]$ and the noise $\overline{w}[n]$ are independent, the pdf of $\overline{y}[n] = \overline{v}[n] + \overline{w}[n]$ can be easily obtained by convolution of the pdfs of $\overline{v}[n]$ and $\overline{w}[n]$. Being the convolution between the Gaussian-like pdf of $\overline{v}[n]$ and the Gaussian mixture pdf of $\overline{w}[n]$, the pdf of $\overline{y}[n]$ can be well approximated by a Gaussian mixture. The obtained approximations for the pdfs of $\overline{v}[n]$, $\overline{w}[n]$, and $\overline{y}[n]$, are then inserted in (10) that, after some computations as in [6], becomes

$$g_{\mathrm{c}}(\overline{y}[n]) = \sigma_v^2 \frac{\sum_{m=0}^{\infty} \frac{\beta_m}{(\sigma_m^2+\sigma_v^2)^{3/2}} e^{-\overline{y}^2[n]/(\sigma_m^2+\sigma_v^2)}}{\sum_{m=0}^{\infty} \frac{\beta_m}{(\sigma_m^2+\sigma_v^2)^{1/2}} e^{-\overline{y}^2[n]/(\sigma_m^2+\sigma_v^2)}} \overline{y}[n], \quad (12)$$

where $\sigma_v^2 = \sigma_y^2 - \sigma_w^2 = \sigma_h^2\sigma_s^2$. Equation (12) provides an MMSE estimate of $\overline{v}[n]$, which, by the Bussgang Theorem, can be decomposed as

$$g_{\mathrm{c}}(\overline{y}[n]) = K\,\overline{v}[n] + \overline{\varepsilon}[n], \quad (13)$$

where $K = E\{g_{\mathrm{c}}(\overline{y}[n])\overline{v}(n)\}/\sigma_{\overline{v}}^2$ is the average gain of the nonlinear estimator, and $\overline{\varepsilon}[n]$ is the residual error, orthogonal to $\overline{v}[n]$. The orthogonality between the useful signal $\overline{v}[n]$ and the residual error $\overline{\varepsilon}[n]$ permits to define the SNR γ as

$$\gamma = K^2\sigma_{\overline{v}}^2/\sigma_{\overline{\varepsilon}}^2, \quad (14)$$

which is related to the MSE J in (9) by

$$\gamma = \frac{K^2\sigma_v^2}{2J - (1-K)^2\sigma_v^2}. \quad (15)$$

B. Cartesian MMSE Soft Limiter Estimator

Alternatively to the nonlinear estimator (12), we can constrain $g(\cdot)$ to have a fixed shape, and design only the parameters of $g(\cdot)$. A popular nonlinear device for impulsive noise reduction is the soft limiter (SL) [5], as expressed by

$$g_{\alpha,\mathrm{SL}}(\overline{y}[n]) = \begin{cases} \overline{y}[n], & \text{if } |\overline{y}[n]| \le \alpha, \\ \mathrm{sgn}(\overline{y}[n])\alpha, & \text{if } |\overline{y}[n]| > \alpha, \end{cases} \quad (16)$$

where α is the threshold to be optimized. Using the approximations discussed in Section III.A, and following the steps in [6], it can be shown that the threshold α that minimizes the MSE $J_{\alpha,\mathrm{SL}} = E\{|\, g_{\alpha,\mathrm{SL}}(\overline{y}[n]) - \overline{v}[n]|^2\}$ is the unique solution of the following fixed-point equation:

$$\alpha = \sigma_v^2 \frac{\sum_{m=0}^{\infty} \frac{\beta_m}{\sqrt{\pi(\sigma_m^2+\sigma_v^2)}} e^{-\alpha^2/(\sigma_m^2+\sigma_v^2)}}{1 - \sum_{m=0}^{\infty} \beta_m \,\mathrm{erf}\left(\alpha/\sqrt{\sigma_m^2+\sigma_v^2}\right)}, \quad (17)$$

where $\mathrm{erf}(x) = 2\pi^{-1/2}\int_0^x \exp(-t^2)dt$ is the error function. Accurate approximations of the exact solution of (17) can be easily found by iterative numerical techniques.

Like (12)–(13), we can exploit the Bussgang Theorem to decompose the SL estimate (16) as

$$g_{\alpha,\mathrm{SL}}(\overline{y}[n]) = K_{\alpha,\mathrm{SL}}\,\overline{v}[n] + \overline{\varepsilon}_{\alpha,\mathrm{SL}}[n], \quad (18)$$

where the average gain $K_{\alpha,\mathrm{SL}}$ can be explicitly calculated as

$$K_{\alpha,\mathrm{SL}} = \sum_{m=0}^{\infty} \beta_m \,\mathrm{erf}\left(\alpha/\sqrt{\sigma_m^2+\sigma_v^2}\right), \quad (19)$$

while the variance of the residual error $\overline{\varepsilon}_{\alpha,\mathrm{SL}}[n]$ in (18) is

$$\sigma_{\overline{\varepsilon},\alpha,\mathrm{SL}}^2 = \sum_{m=0}^{\infty} \beta_m \left\{ \frac{(\sigma_m^2+\sigma_v^2)}{2} \left[\mathrm{erf}\left(\frac{\alpha}{\sqrt{\sigma_m^2+\sigma_v^2}}\right) - \frac{2\alpha e^{-\alpha^2/(\sigma_m^2+\sigma_v^2)}}{\sqrt{\pi(\sigma_m^2+\sigma_v^2)}} \right] + \alpha^2 \left[1 - \mathrm{erf}\left(\alpha/\sqrt{\sigma_m^2+\sigma_v^2}\right) \right] \right\} - K_{\alpha,\mathrm{SL}}^2\sigma_v^2/2. \quad (20)$$

C. MSNR Soft Limiter Estimator

Instead of minimizing the MSE $J_{\alpha,\mathrm{SL}}$, the SL threshold can be optimized in order to maximize the SNR. According to (18) and (14), the SNR is defined as $\gamma_{\alpha,\mathrm{SL}} = K_{\alpha,\mathrm{SL}}^2\sigma_v^2/(2\sigma_{\overline{\varepsilon},\alpha,\mathrm{SL}}^2)$, and its relation with the MSE $J_{\alpha,\mathrm{SL}}$ is the same of (15). Similarly to (17), the SL threshold α that maximizes the SNR $\gamma_{\alpha,\mathrm{SL}}$ can be calculated as the solution of

$$\frac{\sum_{m=0}^{\infty} \beta_m \alpha \left[1 - \mathrm{erf}\left(\frac{\alpha}{\sqrt{\sigma_m^2+\sigma_v^2}}\right) \right]}{K_{\alpha,\mathrm{SL}}^2\sigma_v^2 + 2\sigma_{\overline{\varepsilon},\alpha,\mathrm{SL}}^2} = \frac{\sum_{m=0}^{\infty} \frac{\beta_m e^{-\alpha^2/(\sigma_m^2+\sigma_v^2)}}{\sqrt{\pi(\sigma_m^2+\sigma_v^2)}}}{K_{\alpha,\mathrm{SL}}}, \quad (21)$$

where $K_{\alpha,\mathrm{SL}}$ and $\sigma_{\overline{\varepsilon},\alpha,\mathrm{SL}}^2$ are expressed by (19) and (20), respectively. Equation (21) can be rearranged as a fixed-point equation that can be solved by iterative numerical techniques, like (17). Note that, in general, the solution of (21) is different from that of (17). Therefore, the MSNR threshold for the SL does not coincide with the MMSE threshold for the SL. As a consequence of the different threshold α, the average gain $K_{\alpha,\mathrm{SL}}$ in (19) and the variance $\sigma_{\overline{\varepsilon},\alpha,\mathrm{SL}}^2$ of the residual error in (20) for the MSNR SL estimator are different with respect to those for the MMSE SL estimator.

D. Blanker Estimators

Instead of the SL (16), the function $g(\cdot)$ can be constrained to be a blanking nonlinearity (BN), as expressed by

$$g_{\alpha,\mathrm{BN}}(\overline{y}[n]) = \begin{cases} \overline{y}[n], & \text{if } |\overline{y}[n]| \le \alpha, \\ 0, & \text{if } |\overline{y}[n]| > \alpha. \end{cases} \quad (22)$$

Analogously to the SL of Section III.B, the BN threshold α can be chosen in order to either minimize the MSE or maximize the SNR. Following the steps in [6], the MMSE threshold α for the BN estimator is obtained numerically, by solving

$$\sum_{m=0}^{\infty} \frac{A^m}{m!} \frac{2\sigma_m^2 e^{-\alpha^2/(\sigma_m^2+\sigma_v^2)}}{(\sigma_m^2+\sigma_v^2)^{3/2}} = \sum_{m=0}^{\infty} \frac{A^m}{m!} \frac{e^{-\alpha^2/(\sigma_m^2+\sigma_v^2)}}{(\sigma_m^2+\sigma_v^2)^{1/2}}, \quad (23)$$

whereas the MSNR threshold is obtained by solving

$$\frac{\sum_{m=0}^{\infty} \frac{\beta_m e^{-\alpha^2/(\sigma_m^2+\sigma_v^2)}}{(\sigma_m^2+\sigma_v^2)^{1/2}}}{K_{\alpha,\mathrm{BN}}^2\sigma_v^2 + 2\sigma_{\overline{\varepsilon},\alpha,\mathrm{BN}}^2} = \frac{\sum_{m=0}^{\infty} \frac{2e^{-\alpha^2/(\sigma_m^2+\sigma_v^2)}}{(\sigma_m^2+\sigma_v^2)^{3/2}}}{K_{\alpha,\mathrm{BN}}}, \quad (24)$$

where $K_{\alpha,\mathrm{BN}}$ is the average gain for the BN, expressed by

$$K_{\alpha,\mathrm{BN}} = \sum_{m=0}^{\infty} \beta_m \left[\mathrm{erf}\left(\frac{\alpha}{\sqrt{\sigma_m^2+\sigma_v^2}}\right) - \frac{\sqrt{8}\alpha e^{-\alpha^2/(\sigma_m^2+\sigma_v^2)}}{\sqrt{\pi(\sigma_m^2+\sigma_v^2)}} \right], \quad (25)$$

and $\sigma_{\overline{\varepsilon},\alpha,\mathrm{BN}}^2$ is the variance of the residual error, expressed by

$$\sigma^2_{\bar{\varepsilon},\alpha,\mathrm{BN}} = \sum_{m=0}^{\infty} \beta_m \frac{\sigma_m^2+\sigma_v^2}{2}\left[\mathrm{erf}\left(\frac{\alpha}{\sqrt{\sigma_m^2+\sigma_v^2}}\right) - \frac{2\alpha e^{-\alpha^2/(\sigma_m^2+\sigma_v^2)}}{\sqrt{\pi(\sigma_m^2+\sigma_v^2)}}\right] - \frac{K^2_{\alpha,\mathrm{BN}}\sigma_v^2}{2}. \quad (26)$$

E. Polar Bayesian MMSE Estimator

It is also possible to derive the complex Bayesian MMSE estimator, which jointly works on the I/Q components of the received signal: this estimator would obviously outperform its Cartesian version (12), which does not take into account the dependence of the I/Q impulsive noise components in (3). The problem formulation, as in (10), consists to find

$$g_{\mathrm{mmse}}(y[n]) = E\{v[n] \mid y[n]\} = \int v[n] f_{V|Y}\left(v[n]; y[n]\right) dv[n], \quad (27)$$

where the integral has to be intended as a double integral with respect to the conditional joint pdf of the I/Q components of the complex random variable $v[n] = v_r[n] + jv_i[n]$. Equation (27) can be rewritten likewise (10), and, although we omit the derivations for lack of space, the final result is

$$g_{\mathrm{mmse}}(y[n]) = g_{\mathrm{c}}\left(|\, y[n]\,|\right) e^{j\measuredangle y[n]}, \quad (28)$$

where $y[n] = y_r[n] + jy_i[n] = |\, y[n]\,| e^{j\measuredangle y[n]}$ is the received signal in polar coordinates. This means that the complex MMSE estimator (28) consists of a polar receiver that somehow limits the envelope $|\, y[n]\,|$ of the received signal, while it leaves the phase $\measuredangle y[n]$ unchanged.

The new result (28) may also be considered as a theoretical justification to look for suboptimal polar receivers that simply clip or blank the envelope of the received signal, leaving unchanged the phase, as largely proposed in the literature: for instance, the clipper and blanker of the signal envelope have been proposed in [4] and [5], optimizing the thresholds according to the MSNR criterion, as we did in Sections III.C and III.D for their Cartesian counterparts. The main differences between the SNR maximization of [4], [5], and that in Sections III.C and III.D, are three. First, the optimization of [4] and [5] does not include the multipath channel. Second, the nonlinear devices in [4] and [5] are polar receivers that operate on the complex signal envelope, like (28), thus requiring Cartesian-to-polar conversion stages. Conversely, Cartesian receivers directly operate on the I/Q demodulated components and therefore are slightly simpler. Third, the theoretical analysis for the probability of error, derived in Section IV, turns out to be more accurate than that in [4] and [5], which typically require a very high number of subcarriers (e.g., $N \geq 4096$).

IV. Performance of the Estimators

Using the results in Section III, we can calculate the probability of symbol error on the decision variable $\hat{\mathbf{s}}$ in (4), for both SL and BN estimators. By expressing $\bar{\mathbf{z}} = K\bar{\mathbf{v}} + \bar{\boldsymbol{\varepsilon}}$, where $\bar{\mathbf{z}} = [\bar{z}[0], ..., \bar{z}[2N-1]]^T$, $\bar{z}[n] = g(\bar{y}[n])$, $\bar{\mathbf{v}}$ is defined in (7), and $\bar{\boldsymbol{\varepsilon}} = [\bar{\varepsilon}[0], ..., \bar{\varepsilon}[2N-1]]^T$, we reform the complex vector

$$\mathbf{z} = \mathbf{C}\bar{\mathbf{z}} = K\mathbf{v} + \boldsymbol{\varepsilon}, \quad (29)$$

where $\mathbf{v} = \mathbf{C}\bar{\mathbf{v}}$, $\boldsymbol{\varepsilon} = \mathbf{C}\bar{\boldsymbol{\varepsilon}}$, $\mathbf{C} = [1, j] \otimes \mathbf{I}_N$, and $\otimes$ is the Kronecker product. Using (29) with (2), (4), and (5), we obtain

$$\hat{\mathbf{s}} = \mathbf{s} + K^{-1}\boldsymbol{\Lambda}^{-1}\mathbf{F}\boldsymbol{\varepsilon}, \quad (30)$$

where K is expressed by (19) for the SL and by (25) for the BN, and $\boldsymbol{\varepsilon}$ is the residual noise, with covariance approximately equal to $2\sigma^2_{\bar{\varepsilon},\alpha}\mathbf{I}_N$, where $\sigma^2_{\bar{\varepsilon},\alpha}$ is expressed by (20) for the SL and by (26) for the BN. If the number of subcarriers N is sufficiently high, the frequency-domain residual error $\mathbf{F}\boldsymbol{\varepsilon}$ can be approximated as jointly Gaussian with covariance $2\sigma^2_{\bar{\varepsilon},\alpha}\mathbf{I}_N$. Therefore, the probability of error can be calculated using the classical methods used for AWGN. For square M-QAM, the symbol error probability on the nth subcarrier conditioned on a given channel realization, can be well approximated as $P_{E,n} = 2p_n - p_n^2$, where

$$p_n = \left(1 - \frac{1}{\sqrt{M}}\right)\left[1 - \mathrm{erf}\left(\sqrt{\frac{3\,|\,\lambda_n\,|^2\,\gamma}{2(M-1)\sigma_h^2}}\right)\right], \quad (31)$$

where λ_n is the n th element of the diagonal of $\boldsymbol{\Lambda}$, and the average symbol error probability is $P_E = N^{-1}\sum_{n=0}^{N-1} P_{E,n}$.

V. Simulation Results

In this section, we compare the symbol error rate (SER) performance of the different estimators. We consider the OFDM system of Fig. 1, with $N = 256$ subcarriers, CP length $L = 32$, QPSK data, a Rayleigh fading multipath channel with exponential power-delay profile $\sigma_l^2 = 0.2835\exp(-l/3)$, and a Middleton Class-A noise with $A = 0.01$. With reference to (5), we define the total SNR, which includes both Gaussian and impulsive noise components, as $\mathrm{SNR}_{\mathrm{tot}} = \sigma_s^2/\sigma_w^2$. We also define $\mathrm{SNR}_{\mathrm{imp}} = \mathrm{SNR}_{\mathrm{tot}}(1+T)$, which includes only the impulsive noise component, and $\mathrm{SNR}_{\mathrm{awgn}} = \mathrm{SNR}_{\mathrm{tot}}(1+T)/T$, which includes only the Gaussian noise component. The proposed Cartesian and polar receivers (12), (16), (22), (28), identified by the suffixes "Cart" and "Pol" in the figure legends, are compared with the classical linear least-squares (LS) equalizer that does not employ any kind of impulsive noise reduction, and with the MSNR SL and BN polar estimators. Note that according to Fig. 1, and differently from [3], also the MSNR SL and BN polar estimators are applied before the channel equalizations, and adapt their thresholds to the channel state.

Fig. 2 compares the SER performance of the proposed estimators as a function of the total SNR, $\mathrm{SNR}_{\mathrm{tot}}$, when $T = 0.01$. Fig. 2 proves that the proposed estimators are effective, especially at low SNR. The Bayesian MMSE estimator and the BN estimators provide the best SER, followed by the SL estimators. Specifically, in this simulation scenario, MMSE estimators yield the same performances of MSNR estimators. As expected, the polar estimators, which act on the signal envelope, yield slightly better performance than their Cartesian counterparts based on the I/Q components, which however are slightly less complex. Also note that the theoretical SER curves well match the simulated SER, for both Cartesian and polar SL and BN estimators.

Fig. 3 shows the SER of the proposed estimators as a function of the impulsive-noise SNR, $\mathrm{SNR}_{\mathrm{imp}}$, when the Gaussian-noise SNR is $\mathrm{SNR}_{\mathrm{awgn}} = 20$ dB. Also in this scenario, the Bayesian MMSE and the BN are the best estimators. Fig. 4 exhibits the SER of the proposed estimators as a function of the Gaussian-noise SNR $\mathrm{SNR}_{\mathrm{awgn}}$, when the impulsive-noise SNR is $\mathrm{SNR}_{\mathrm{imp}} = -20$ dB. Note that, when $\mathrm{SNR}_{\mathrm{awgn}}$ is quite low, MSNR estimators outperform MMSE estimators. This is consistent with the SER analysis, since the probability in (31) depends on the SNR.

VI. Conclusions

We have investigated sample-based MMSE and MSNR Class-A noise mitigation techniques for wireless OFDM systems in frequency-selective fading channels. We have also proposed a semi-analytical SER performance assessment that turns out to be quite accurate for both Cartesian-based receivers and polar-based receivers. Future work will deal with the design of channel estimators that are robust to impulsive noise.

References

[1] M. Ghosh, "Analysis of the effect of impulse noise on multicarrier and single carrier QAM systems," *IEEE Trans. Commun.*, vol. 44, no. 2, pp. 145–147, Feb. 1996.

[2] H. Nikookar and D. Nathoeni, "Performance evaluation of OFDM transmission over impulsive noisy channels," *IEEE Int. Symp. Personal, Indoor Mobile Radio Commun. (PIMRC),* 2002.

[3] S. V. Zhidkov, "Impulsive noise suppression in OFDM-based communication systems," *IEEE Trans. Consum. Electron.*, vol. 49, no. 4, pp. 944–948, Nov. 2003.

[4] S. V. Zhidkov, "Performance analysis and optimization of OFDM receiver with blanking nonlinearity in impulsive noise environment," *IEEE Trans. Veh. Technol.,* vol. 55, no. 1, pp. 234–242, 2006.

[5] S. V. Zhidkov, "Analysis and comparison of several simple impulsive noise mitigation schemes for OFDM receivers," *IEEE Trans. Commun.,* vol. 56, no. 1, pp. 5–9, Jan. 2008.

[6] P. Banelli, "Bayesian estimation of a Gaussian source in Middleton's class-A impulsive noise," IEEE *Signal Process. Lett.,* vol. 20, no. 10, pp. 956–959, Oct. 2013.

[7] D. Middleton, "Statistical-physical models of urban radio-noise environments–Part I: Foundations," *IEEE Trans. Electromagn. Compat.,* vol. 14, no. 2, pp. 38–56, May 1972.

[8] D. Middleton, "Non-Gaussian noise models in signal processing for telecommunications: new methods an results for class A and class B noise models," *IEEE Trans. Inf. Theory*, vol. 45, no. 4, pp. 1129–1149, May 1999.

[9] L. Berry, "Understanding Middleton's canonical formula for class A noise," *IEEE Trans. Electromagn. Compat.,* vol. 23, no. 4, pp. 337–344, Nov. 1981.

[10] D.-F. Tseng, Y. S. Han, W. H. Mow, L.-C. Chang, and A. J. H. Vinck, "Robust clipping for OFDM transmissions over memoryless impulsive noise channels," IEEE *Commun. Lett.,* vol. 16, no. 7, pp. 1110–1113, July 2012.

[11] F. H. Juwono, Q. Guo, Y. Chen, L. Xu, D. Huang, and K. P. Wong, "Linear combining of nonlinear preprocessors for OFDM-based power-line communications," *IEEE Trans. Smart Grid*, in press.

[12] Y.-H. Kim, K.-H. Kim, H.-M. Oh, K.-H. Kim, and S.-C. Kim, "Mitigation of effect of impulsive noise for OFDM systems over power line channels," *IEEE Int. Symp. Power Line Commun. Applicat. (ISPLC),* 2008.

[13] A. Mengi and A. J. H. Vinck, "Successive impulsive noise suppression in OFDM," *IEEE Int. Symp. Power Line Commun. Applicat. (ISPLC),* 2010.

[14] J. Lin, M. Nassar, and B. L. Evans "Impulsive noise mitigation in powerline communications using sparse Bayesian learning," *IEEE J. Sel. Areas Commun.*, vol. 31, no. 7, pp. 1172–1183, July 2013.

[15] J. Armstrong and H. A. Suraweera, "Impulse noise mitigation for OFDM using decision directed noise estimation," *IEEE Int. Symp. Spread Spectrum Techniques Applicat. (ISITA),* 2004.

[16] F. Abdelkefi, P. Duhamel, and F. Alberge, "Impulsive noise cancellation in multicarrier transmission," *IEEE Trans. Commun.,* vol. 53, no. 1, pp. 94–106, Jan. 2005.

[17] C.-H. Yih, "Iterative interference cancellation for OFDM signals with blanking nonlinearity in impulsive noise channels," *IEEE Signal Process. Lett.,* vol. 19, no. 3, pp. 147–150, Mar. 2012.

[18] G. Caire, T. Y. Al-Naffouri, and A. K. Narayanan, "Impulse noise cancellation in OFDM: an application of compressed sensing," *IEEE Int. Symp. Inf. Theory (ISIT),* 2008.

[19] K. S. Al-Mawali and Z. M. Hussain, "Adaptive-threshold clipping for impulsive noise reduction in OFDM-based power line communications," *IEEE Int. Conf. Advanced Technol. Commun. (ATC),* 2009.

[20] H. Oh, H. Nam, and S. Park, "Adaptive threshold blanker in an impulsive noise environment," *IEEE Trans. Electromagn. Compat.,* vol. 56, no. 5, pp. 1045–1052, Oct. 2014.

[21] P. Banelli, "Non-linear transformations of gaussians and gaussian-mixtures with implications on estimation and information theory," submitted for publication. Available: http://arxiv.org/abs/1111.5950v3.

[22] Z. Wang and G. B. Giannakis, "Wireless multicarrier communications," *IEEE Sig. Proc. Mag.*, vol. 17, no. 3, pp. 29–48, May 2000.

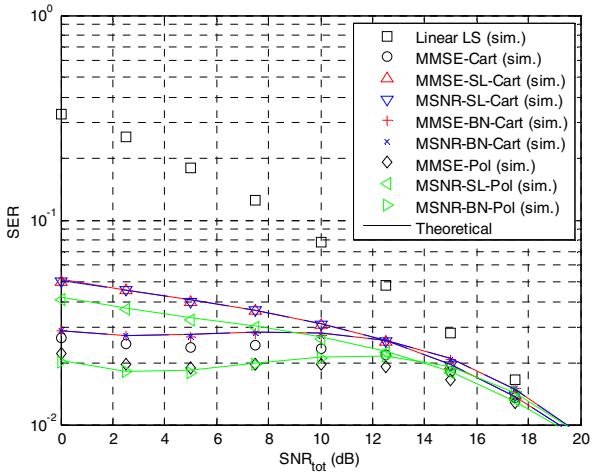

Fig. 2. SER comparison as a function of the total SNR.

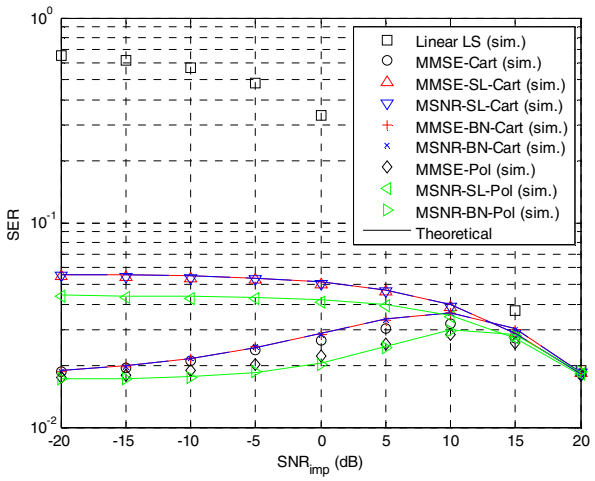

Fig. 3. SER comparison as a function of the impulsive-noise SNR.

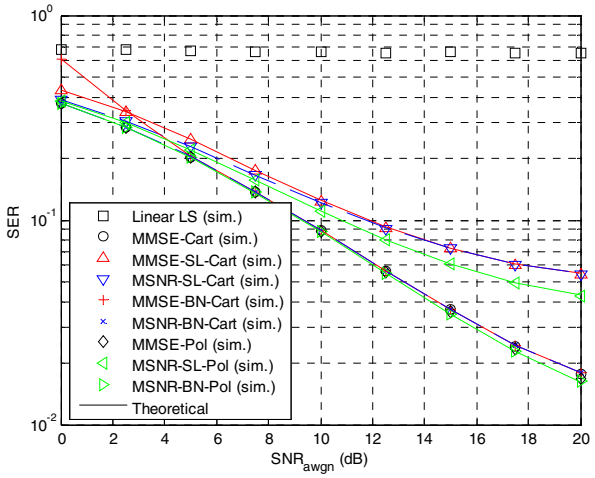

Fig. 4. SER comparison as a function of the Gaussian-noise SNR.